Supporting Information

Synergistic Interface Engineering of $Co(OH)_2$@AgNPs Heterojunction for Trace Electrochemical Hg^{2+} Detection

Yanchao Sun, Hongliang Dai, Zheng Wang Weiqiang Fan*, Hongye Bai*

Calculation of Limit of Detection (LOD) and limit of quantification (LOQ)

The Limit of Detection (LOD) and limit of quantification (LOQ) of the $Co(OH)_2$@AgNPs sensor for Hg^{2+} was calculated based on the standard signal-to-noise ratio equation (S/N = 3, S/N = 10), following the IUPAC guidelines. The calculation formula is as follows:

$$LOD = \frac{3\sigma}{S}$$

$$LOQ = \frac{10\sigma}{S}$$

Where:

- σ represents the standard deviation of the blank response. It was derived by measuring the peak current of the blank electrolyte (0.5 M Na_2SO_4 without Hg^{2+}) for 10 consecutive measurements.
- *S* represents the sensitivity of the sensor, corresponding to the slope of the linear calibration curve (Fig. 5) in the low concentration range.

In this work, the standard deviation (σ) was determined to be 0.0084 μA, and the slope (S) was obtained from the linear regression equation (y = 0.02972x + 0.07245) as 0.02972 μA nM^{-1}. Consequently, the LOD was calculated to be 0.85 nM, LOQ was calculated to be 283 nM.

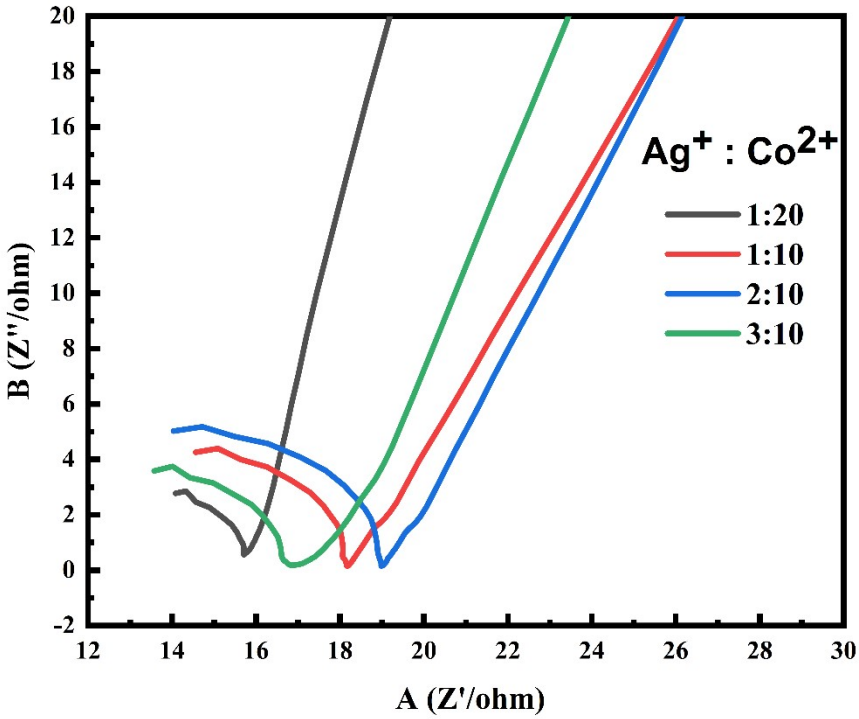

Fig S1. EIS comparison of FTO/$Co(OH)_2$@AgNPs prepared from deposition solutions at different ratios.

Table S1: Comparison of Electrochemical Parameters for FTO/$Co(OH)_2$@AgNPs Prepared at Different Ag^+:Co^{2+} Deposition Ratios

Ag^+:Co^{2+} Deposition Ratio	Curve Color	Solution Resistance (Rs / Ω)	Charge Transfer Resistance (R_{ct} / Ω)	Conductivity Evaluation
1:20	Black	≈11.2	≈5.5	Low/Medium
1:10	Red	≈11.4	≈8.5	High
2:10	Blue	≈11.3	≈4.8	Good
3:10	Green	≈11.1	≈2.5	Excellent

Note: The R_{ct} values are estimated based on the semicircle diameter read from the Nyquist plot (not precisely measured).

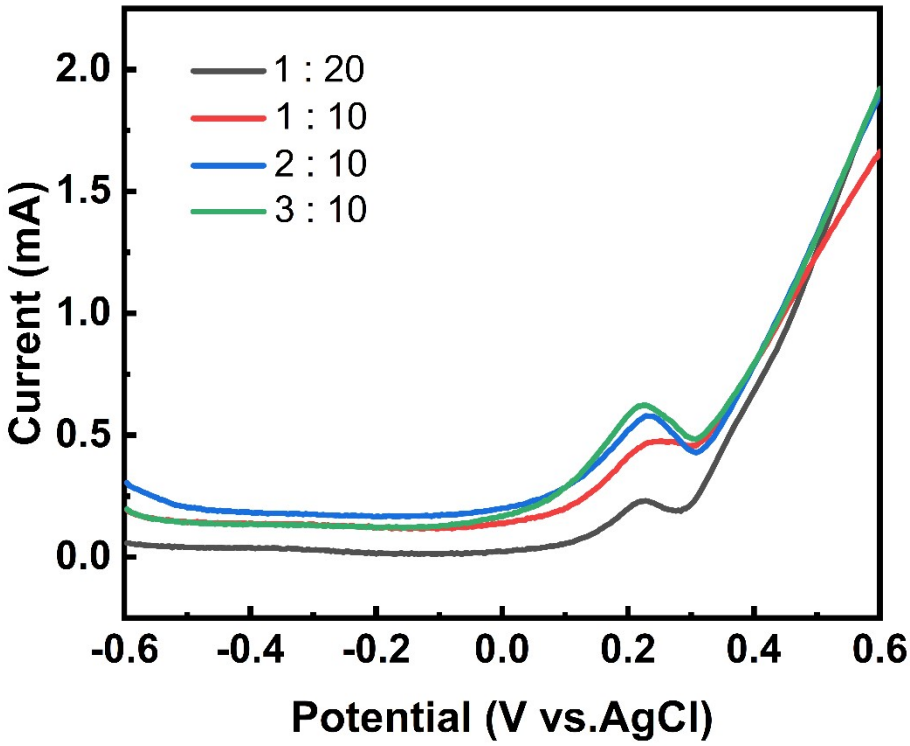

Fig S2. Comparison of SWV for $Co(OH)_2$@AgNPs prepared from sedimentation solutions at different ratios.

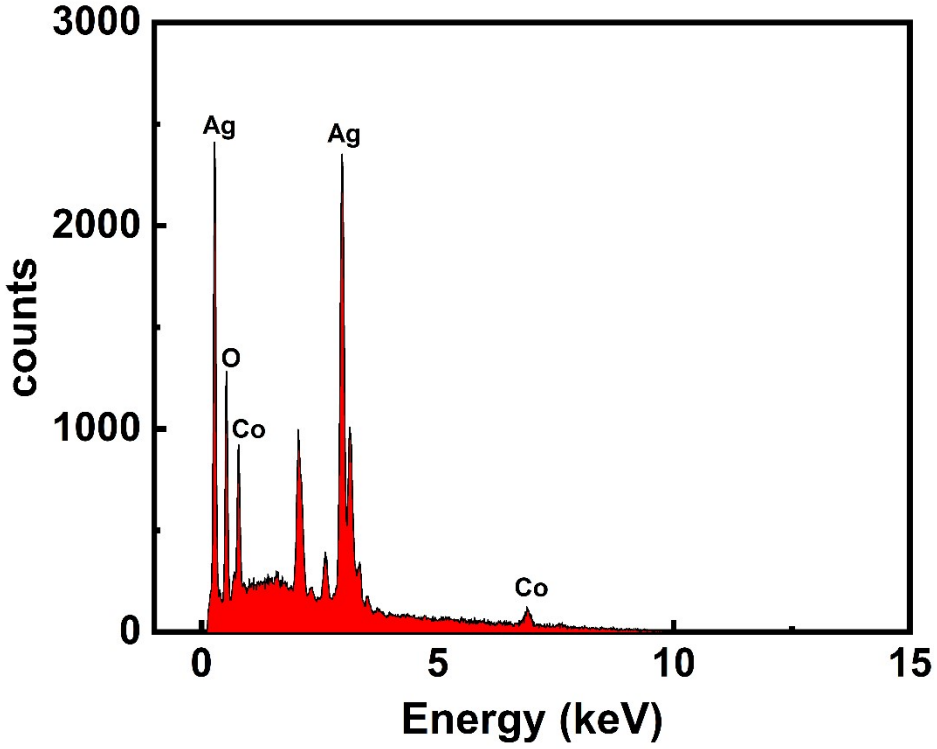

Fig S3. EDS spectrum of $Co(OH)_2$@AgNPs.

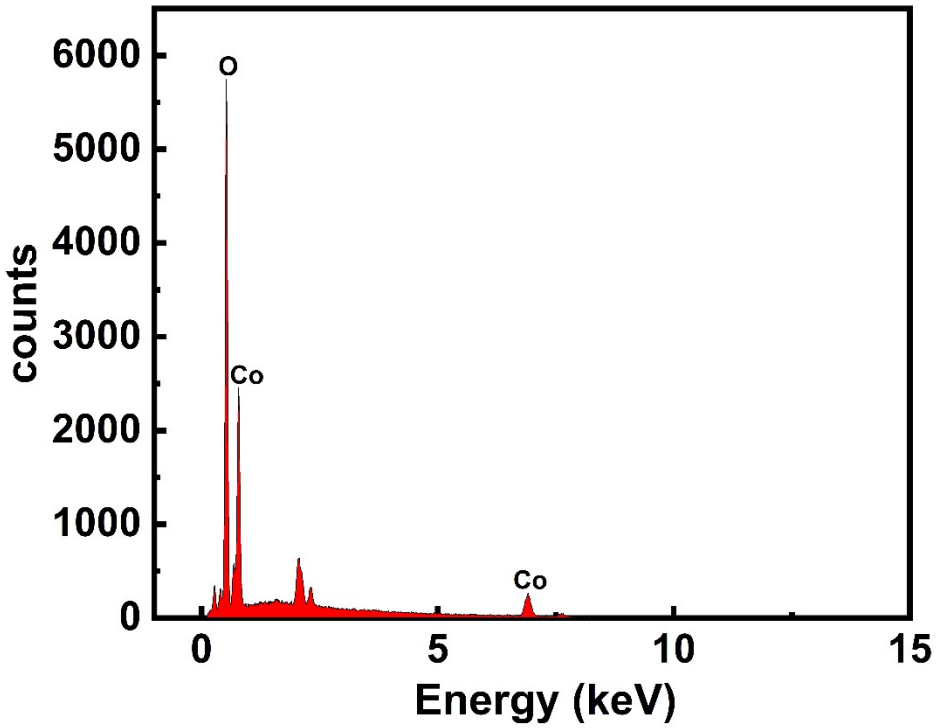

Fig S4. EDS spectrum of $Co(OH)_2$**.**

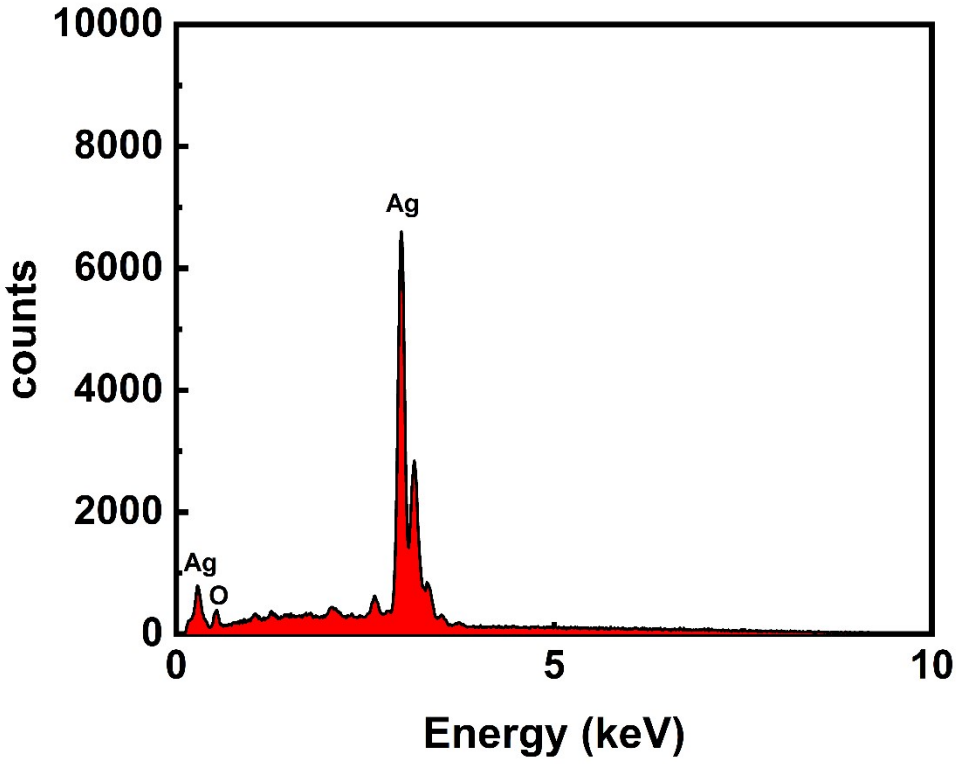

Element	Mass Norm.[%]	Atom.[%]
Ag	98.444	90.36985
O	1.556001	9.630151
—	100	100

Fig S5. EDS spectrum and elemental composition analysis of silver-based material.

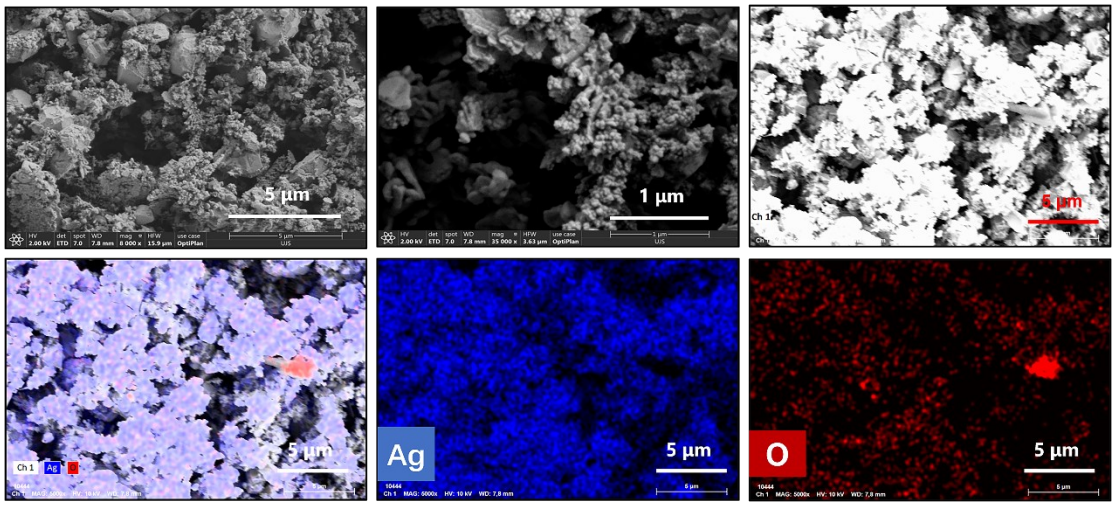

Fig S6. SEM and elemental distribution of AgNPs.

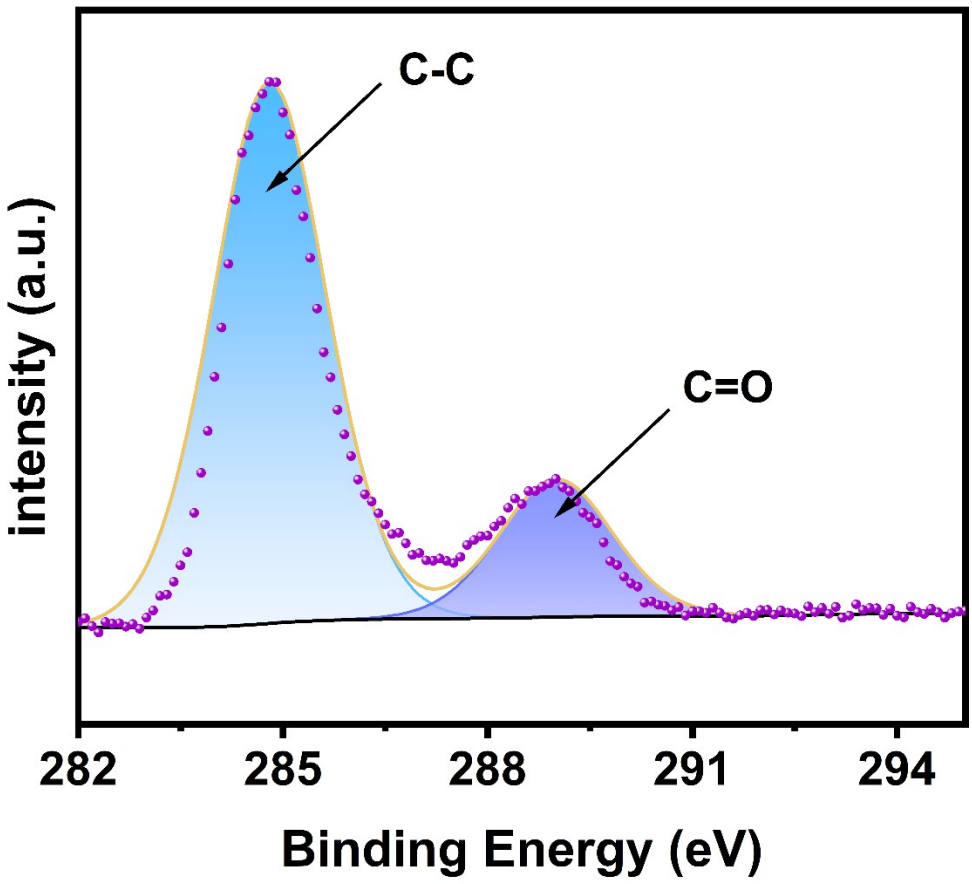

Fig S7. High-resolution XPS spectrum of the C 1s region.

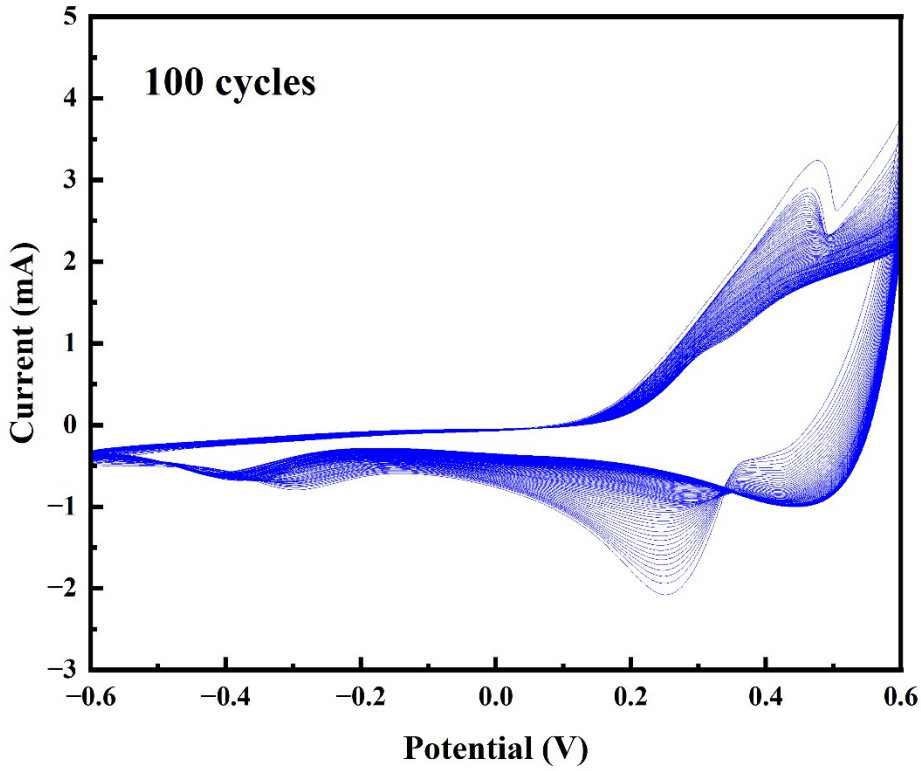

Fig S8. 100-cycle CV of $Co(OH)_2$@AgNPs.

Table S2. Theoretical selectivity mechanism based on HSAB and hydration energy [1-6].

Ion	Classification	Theoretical Affinity to Ag	Selectivity Response	Mechanism
Hg^{2+}	Soft acid	High / Spontaneous	Strong response	Soft acid–soft base interaction, forming $AgHg_3$ alloy
Pb^{2+}	Borderline acid	Low	Weak/very weak response	Weak orbital overlap, no alloy formation
Cd^{2+}	Borderline acid	Low	Weak/very weak response	High solvation energy shielding
Cu^{2+}	Borderline acid	Negligible	Weak/very weak response	Jahn-Teller distortion-induced bond weakening
Zn^{2+}	Hard acid	Negligible	No response	Strong hydration shell screening
Ni^{2+}	Hard acid	Negligible	No response	High crystal field stabilization energy

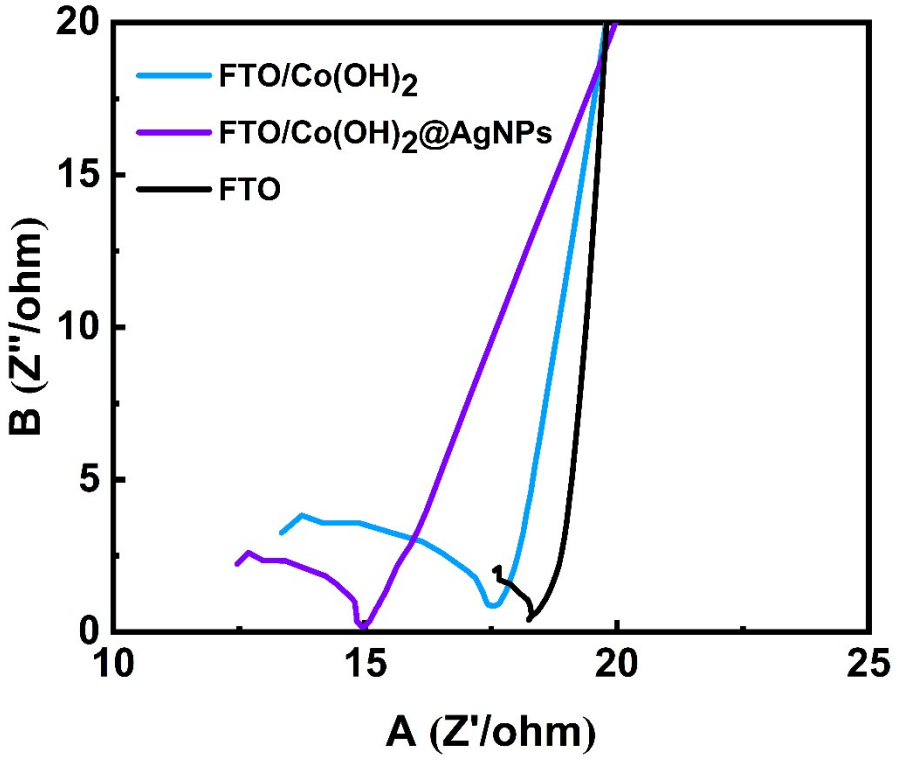

Fig S9. EIS comparison of blank FTO, FTO/$Co(OH)_2$, and FTO/$Co(OH)_2$@AgNPs.

Table S3. Comparative Electrochemical Performance of FTO, FTO/$Co(OH)_2$ and FTO/$Co(OH)_2$@AgNPs Electrodes

Parameter	FTO	FTO/$Co(OH)_2$	FTO/$Co(OH)_2$@AgNPs
Estimated R_{ct} (Ω)	~18 Ω	~14 Ω	~10 Ω
Charge transfer ability	Poor	Moderate	Excellent
Electrocatalytic activity	Low	Medium	High
Interfacial resistance	High	Medium	Low
Modification effect	—	Improved	Significantly improved

Note: The R_{ct} values are estimated based on the semicircle diameter read from the Nyquist plot (not precisely measured).

Table S4. Size-Sieving Effect of Layered $Co(OH)_2$ (Interlayer Spacing = 0.46 nm)[7, 8]

Substance	Characteristic Size (nm)	Can Enter Interlayer?	Sieving Effect
Hg^{2+}	0.112 (ionic radius)	Yes	No barrier
Cd^{2+}	0.109 (ionic radius)	Yes	Partial entry
Pb^{2+}	0.133 (ionic radius)	Yes	Partial entry
Parathion	>1.2 (molecular size)	No	Complete blocking
AsO_4^{3-}	0.46 (hydration radius)	Critical restriction	Significant hindrance
Protein molecules	>3.0 (molecular size)	No	Complete blocking

Table S5. The recovery rate of Hg^{2+} at different concentrations in river water.

Background Value (nM)	Spiked Amount (nM)	Measured Value (nM)	Recovery (%)	RSD (%)	Pretreatment Method
ND	15	14.7	98.0	3.2	0.45 μm filtration, pH 7.0
—	50	51.1	102.2	2.5	—
—	100	98.5	98.5	1.8	—

***Notes*:**

1. **ND:** Not detected (below LOD = 0.85 nM).
2. **Recovery calculation formula:** Recovery (%) = [(Measured value – Background value)/Spiked amount] × 100%.
3. **RSD:** Relative standard deviation from three parallel experiments (n = 3), reflecting method precision.
4. **Pretreatment:** All water samples were filtered through a 0.45 μm membrane to remove suspended particles, and the pH was adjusted to 7.0 (consistent with the electrolyte) using 0.1 M $NaOH/H_2SO_4$.

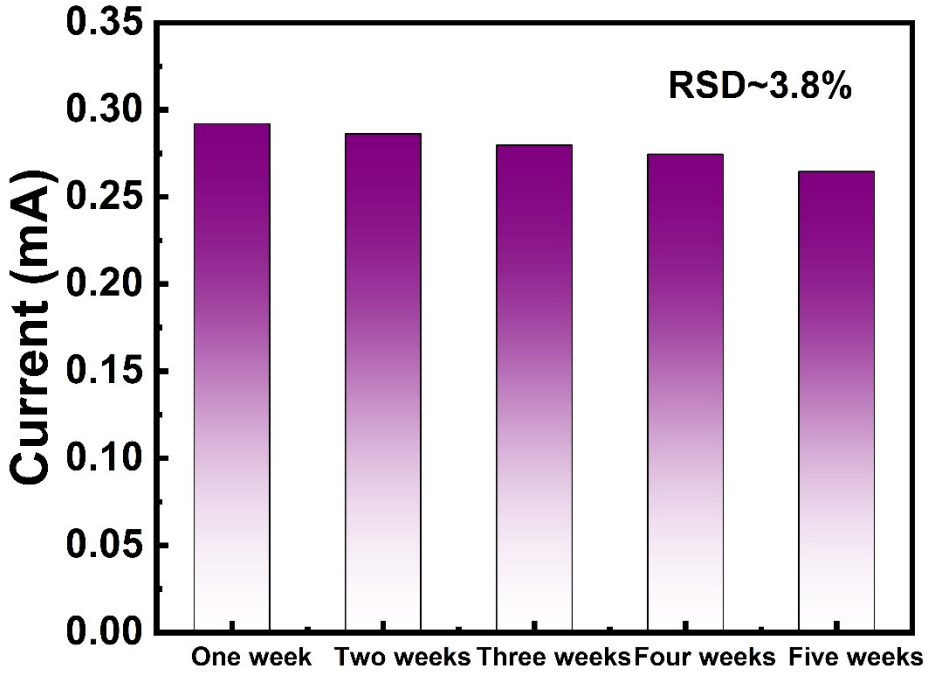

Fig S10. Long-term stability of the FTO/$Co(OH)_2$@AgNPs sensor stored over 5 weeks. (The concentration of Hg^{2+}: 100 nM)

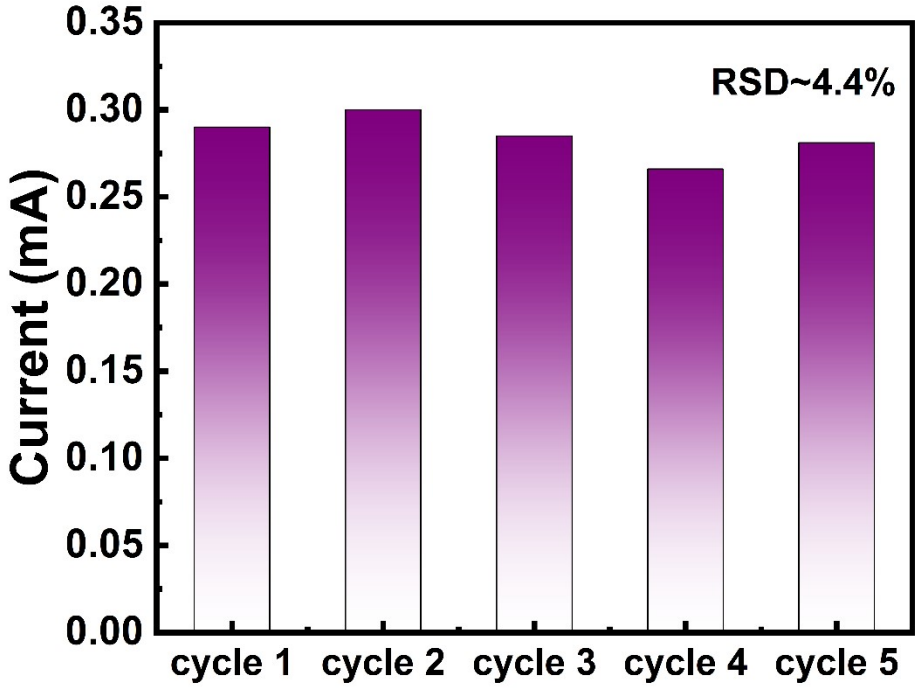

Fig S11. Repeatability of the sensor for five successive measurements on a single electrode. (The concentration of Hg^{2+}: 100 nM)

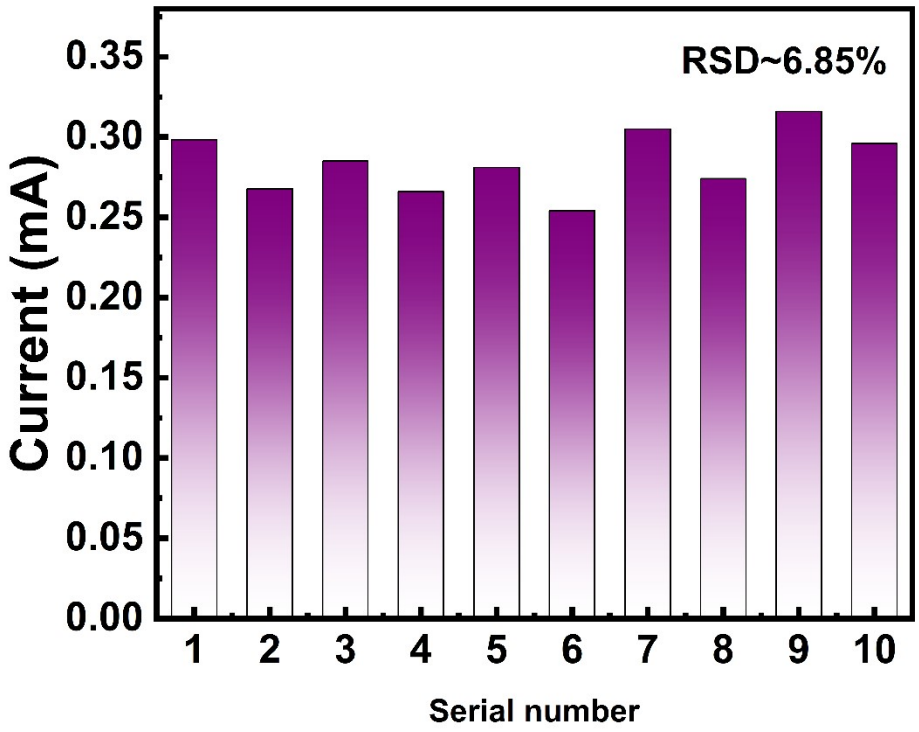

Fig S12. Reproducibility of ten independently fabricated electrodes. (The concentration of Hg^{2+}: 100 nM)

References

[1] W. Sachtler, "Chemisorption complexes on alloy surfaces," *Catalysis Reviews—Science and Engineering,* vol. 14, no. 1, pp. 193-210, 1976.

[2] J. A. Steckel, "Density functional theory study of mercury adsorption on metal surfaces," *Physical Review B—Condensed Matter and Materials Physics,* vol. 77, no. 11, p. 115412, 2008.

[3] M. Akbari, "Adsorption of MCl2 (M= Hg, Cd, and Pb) on CuS (001) surface. Density functional theory study," *Environment Protection Engineering,* vol. 51, no. 2, 2025.

[4] G. A. Bodkhe, B. Hedau, M. S. More, M. Kim, and M. D. Shirsat, "Electrochemical Sensing of Hg^{2+} Ions Using an SWNTs/Ag@ ZnBDC Composite with Ultra-Low Detection Limit," *Chemosensors,* vol. 13, no. 7, p. 259, 2025.

[5] H. Chen, X. Yang, Y. Li, and J. Chen, "A Density Functional Theory Study on the Effects of Silver Doping on the Properties and Flotation Behavior of Jamesonite," *Molecules,* vol. 30, no. 7, p. 1424, 2025.

[6] Y. Yang *et al.*, "A highly selective and sensitive nano-silver sol sensor for Hg^{2+} and Fe3+: green preparation and mechanism," *Polymers,* vol. 14, no. 18, p. 3745, 2022.

[7] Y. Marcus, "Ionic radii in aqueous solutions," *Chemical Reviews,* vol. 88, no. 8, pp. 1475-1498, 1988.

[8] X. Wu *et al.*, "Electrodeposition-potential tuning rejuvenates the concurrent preparation from α-Co (OH) 2 with larger interlayer-spacings to β-Co (OH) 2," *Batteries & Supercaps,* p. e202400699, 2025.